Mechanics of Advanced Composite Structures

Journal homepage: https://macs.semnan.ac.ir/

Semnan University

ISSN: 2423-7043

Research Article

Experimental Analysis of the Effect of Mechanical Topology on the Surface of Biological Microgripper Made of Ionic-Polymer Metal Composite Smart Material

Hamid Soleimanimehr [a,b]*, Shadan Bafandeh Haghighi [a,b], Amin Nasrollah [c]

[a] *Department of Mechanical and Aerospace Engineering, SR.C., Islamic Azad University, Tehran, Iran*

[b] *Modern Automotive Research Center, SR.C., Islamic Azad University, Tehran, Iran*

[c] *Department of Mechanical Engineering, Iran University of Science and Technology, Tehran, Iran*

ARTICLE INFO

Article history:

Received: 2024-04-29
Revised: 2024-10-09
Accepted: 2024-12-18

Keywords:

Ionic polymer metal composite (IPMC);
Bio-Compatibility;
Blocking force;
Finite element method;
Experimental method.

ABSTRACT

This paper aims to discuss the electromechanical behavior of an ionic polymer metal composite (IPMC) with electrodes made of platinum and polymeric membrane made of Nafion-117 in the structure of a gripper. Two methods are used in this research; the experimental method and the finite element method. After producing an IPMC with the mentioned properties and setting the gripper structure, the generated blocking force was measured and its ability to lift and move two external specimens made of aluminum and fish egg with a radius of $8.23 \times 10^{-4}\ m$ m was evaluated. The Same analysis was done by the finite element method. The magnitude of the distributed load is approximately equal to 590 N/m^2. The surface area of the sample is equal to 115 mm^2. After conducting the statistical calculations, the concentrated force on the tip of the beam is $52.95 \times 10^{-3}\ N$ and the results of the two methods are consistent with each other with an error of 0.092 %. When a concentrated force is applied to the spherical sample, both pure aluminum and fish egg materials experience an identical maximum stress of 9.97 MPa. The maximum displacement for the aluminum sample is 0.613 μm, and for the fish egg sample, it is 2.62 μm. It has been concluded that this gripper is able to lift and move the mentioned samples and IPMC is a biocompatible material since it is compatible with the bio-sample (fish egg) considered in this research.

1. Introduction

Generally, devices that do the conversion of applied energy to motion are called actuators. The traditional complicated actuators like metallic and ceramic ones which were used in different mechanisms were not adopted in biomedical systems, but polymeric actuators are more biocompatible in contrast to them. Lightweight, simplicity, fast responsibility, silence, and biodegradability are some of the polymeric actuators' advantages. The polymeric actuators change in size and shape in response to actuation and these changes are controllable [1].

Electroactive polymer-based actuators are one of the main types of actuators. The mechanical or optical characteristics of EAPs change in response to an electric field and the transformation from electrical to mechanical

* **Corresponding author.**
E-mail address: Ha.sol@iau.ac.ir

Cite this article as:

Soleimanimehr, H., Bafandeh Haghighi, Sh. and Nasrollah, A., 2026. Experimental Analysis of the Effect of Mechanical Topology on the Surface of Biological Microgripper Made of Ionic- Polymer Metal Composite Smart Material. *Mechanics of Advanced Composite Structures*, 13(1), pp. 143-156.

https://doi.org/10.22075/MACS.2024.33962.1670

energy and vice versa could be accurately controlled. By representing a good potential actuation strain, good scalability, and low cost, EAPs are good candidates for applications such as sensors and artificial muscles [2].

Electroactive muscles are divided into two groups: dielectric and ionic EAPs. Dielectric elastomers, ferroelectric polymers, electro-strictive graft elastomers, and liquid crystal elastomers are instances of dielectric EAPs and ionic EAPs are divided into three subbranches; ionic polymer gels, conductive polymers, and ionic polymer metal-composites (IPMCs) [3].

As mentioned, ionic polymer metal-composites are a main subset of the big group of electroactive polymers and are known as smart materials consisting of three layers; an ionic polymer sheet which is typically Nafion or Flemion, and two layers of coated electrodes from noble metals like platinum and gold [4].

As an actuator, IPMCs show deformation under small amounts of applied voltages and on the other hand, generate a small amount of voltage when deformed. These smart materials are applicable in various fields as actuators, sensors, and energy harvesters; also, IPMCs are biocompatible materials, and using them as artificial muscles is one of their significant applications [5].

Different methods of coating electrodes are applicable in the procedure of manufacturing IPMCs. Hot pressing (HP), Solution Casting (SC), Sputtering Deposition (SD), Electroless plating, Electroplating, and Direct assembly process (DAP) are common methods of coating used in IPMC manufacturing. Two important factors must be considered despite of method being used; the electrode particles must be spread as widely as possible through the surface of the polymer so the maximum interface with the polymer layer be provided, and the coating region must be as near as possible to the surface of the polymer layer and not in high depth [6].

A commonly used method for solving practical problems is the finite element method (FEM). This method estimates and controls the errors of the solution approximation, based on quantitative data. This method can be described as a key member of predictive computational science including verification of codes and solutions, definition of statistical sub-models, calibration and verification of models, formulation of mathematical models, and forecasting of the behavior of physical models by considering specific uncertainties [7].

IPMC analysis by finite element method includes parameters that affect its electromechanical and mechanoelectrical behavior. In the continuation of the discussion, we will briefly introduce these parameters. "The diffusion coefficient" is a measure of particles or molecules' dispersion or diffusion quickness through a medium. It defines the proportionality between the flux of particles and the concentration gradient. This parameter depends on various factors and relates to different phenomena. It is commonly expressed in units of squared meters per second. (m^2/s)In the International System of Units (SI) [8].

In the context of IPMC analysis, "concentration" typically refers to the amount of cation that has been dissolved in the ionic polymer membrane; and generally, concentration is the amount of solute being dissolved in a solvent [9].

"The charge number" is a quantized amount of electric charge (q). The quantum of electric charge is the elementary charge (e). In other words, it could be defined as the measure of lack or excess of the elementary charge in a charged particle as a positive or negative amount. The following equation provides the amount of charge number: $z = q/e$ [10].

Faraday constant is a physicochemical constant defined as the amount of electrical charge carried by one mole of electrons or one mole of singly charged ions. This constant is named after Michael Faraday, a British scientist in the field of electricity and electrochemistry. The Faraday constant is precisely determined as $F = N_A.e$ which N_A is Avogadro's constant and e is the elementary charge[11].

In a simple word, permittivity is an electromagnetism parameter that determines how a dielectric material becomes polarized in response to the external electric field. The more permittivity amount the more energy being stored in the material. It is denoted by the symbol ε and the SI unit for it is Farad per meter (F/m)[12].

At a specific temperature, The ratio of a substance's mass (kg) to its volume (m^3) is known as the density of the material. The SI unit of this parameter is (kg/m^3) or (g/cm^3) and it is denoted by the symbol ρ [13].

Elastic materials show a linear relationship between the applied normal stress and the corresponding normal strain caused by that. The slope of this linear relationship is Young modulus, named after a British scientist, Thomas Young. It is denoted by the symbol E and represents the stiffness of a material. It quantifies how much a material will deform when subjected to a given amount of stress [14].

Dividing the axial strain by lateral strain when a sample of material is stretched or compressed, provides a mechanical property known as Poisson's ration. This parameter represents how a specific material responds to

deformation and it is useful in mechanical design [15].

The structure of IPMCs consists of an ion-exchange polymeric membrane which is mostly cation-exchange and two metallic electrode layers deposited on both surfaces of the membrane. The mechanical properties of the IPMC are mainly related to the ionomeric membrane. More precisely, the actuation mechanism occurs when together clustered anions inside the polymeric membrane, provide channels for flow of the cations. When a specific amount of voltage (commonly 1-5 volts) is applied to the electrodes, aggregation of hydrated cations on the negative electrode side causes mechanical and electrostatic stress, which translates into the IPMC actuator's deformation [16].

The mechanoelectrical behavior of IPMCs makes them applicable as sensors. When a variation in environmental factors such as humidity, PH rate, or temperature occurs, the deformation of IPMC results in changes in their electrical properties. Precise and responsive detection of environmental and physical parameters is possible due to these sensing capabilities of IPMCs. Unique advantages of this smart material such as its lightweight nature, flexibility, and biocompatibility extend its utility in various fields of engineering, medication, and environmental monitoring [17].

Previous research on IPMC actuators has utilized the FEM method to simulate mathematical models for precise predictions of actuation force and displacement. Key factors in this process included frequency, applied voltage, and material compositions. One notable innovation is the IPMC microgripper, capable of handling micro-scale components without conventional motors. A particularly novel approach involves an IPMC-based microgripper controlled by EMG signals from human fingers, showing potential for tasks such as pin insertion during robotic micro-assembly. Another study designed a porous IPMC actuator with microchannels and nanopores in the Nafion membrane, enhancing ionic liquid absorption and resulting in increased capacitance and stability over prolonged use.

2. Material and Methods

2.1. Ionic-Polymer-Metal-Composites Producing Method

As mentioned before, two methods of analysis are used in this article; the experimental method and the Finite element method. The production of an ionic polymer metal-composite sample used in experimental analysis is the first step in this research.

The surface of the polymeric membrane of Nafion-117 is roughened by initial sandblasting so that better electrode coating on the surface of the polymer can be achieved. Soft glass beads are shot on the surface, by the pressure of compressed air. This procedure is done to prepare the polymeric membrane for better coating of metallic electrodes [18].

After sandblasting the Nafion layer, it is time to wash the membrane with an ultrasonic washer. This causes the residual particles, oils, and dust to be eliminated from the Nafion layer. The presence of impurities in the membrane causes a disruption in the bond between the polymer matrix and metallic electrodes; weak cohesion between the composite layers and reduced function of IPMC are the results of ignoring this foulness. Another outcome of using an ultrasonic washer is that it activates metallic particles; especially gold and platinum. This method of cleansing is quicker and more efficient in comparison with other chemical and manual methods [19].

Treatment of the membrane with hydrochloric acid (HCl) is the next step. In this phase of treatment, we should boil the membrane in a solution of HCl and then rinse it with deionized water. Omission of impurities and residuals, increasing the activation of metallic particles, and improvement of electrochemical properties of metallic electrodes such as conductivity and catalytic activity are the advantages of HCl treatment that results in more efficient charge transfer between electrode and electrolyte [20].

After preparing the polymeric membrane by the above-mentioned process, the next step is "adsorption" or in other words, "ion exchange". A compound of platinum, like $[Pt(NH_3)_4Cl_2]$ or $[Pt(NH_3)_6Cl_4]$ is needed. A solution of Ammonium hydroxide of (5-10)% wt. concentration should be prepared. We place the treated membrane in a solution of a platinum compound and leave it for at least three hours; the Ammonium hydroxide solution should be gradually added during this time. The amount of absorption depends on the amount of electric charge; The greater the charge, the better absorption occurs [21].

Primary plating starts by preparing a (5-10)% wt solution of $NaBH_4$ and a water bath of 4 0°C. After absorption, we place the polymeric membrane in an amount of steering water and then put it in the prepared water bath. $NaBH_4$ solution should be added every 30 minutes in 7 sequences. During this process, we gradually raise the temperature of the water bath to 80 °C. Finally, we add some amount of

$NaBH_4$ solution and stir it for an hour and a half at 80 °C. Black platinum particles start to appear on the surface of Nafion. Washing the prepared composite with deionized water and then putting it into a dilute HCl solution is the final step for primary plating [22].

Secondary plating needs the same solutions used in primary plating; a $(5-10)$ % solution of $NH_2OH-HCl$ and a 25 % solution of NH_2NH_2 are needed too. We put the composite in a stirring solution of platinum at 40°C. During four hours the temperature of the solution must be gradually increased to 80°C and specific amounts of Hydroxylamine hydrochloride and Hydrazine solutions must be added every 30 minutes [23].

To make sure that all mounts of platinum have been coated on the composite, we boil the membrane in a solution of $NaBH_4$. It is so important to notice that $NaBH_4$ should not be added to a hot solution because there is a hazard of a gas explosion. As the final step, the composite is washed with dilute. HCl solution to omit the Ammonium cations in the membrane and then it is washed with deionized water [24].

2.2. Experimental Analysis

The electromechanical behavior of IPMC as an actuator has been analyzed in this research. For verification and comparison, this analysis has been done by two methods; the experimental method and the finite element method. In this section, we are going to explain the experimental analysis of the material's behavior.

The Ionic polymer metal-composite deforms under the influence of an external electrical field applied to the surface of its electrodes, and this deformation is influenced by supportive constraints and IPMC's initial shape. The mentioned deformation caused by electrical excitation appears as the result of the generated force called the "Blocking force" of the IPMC.

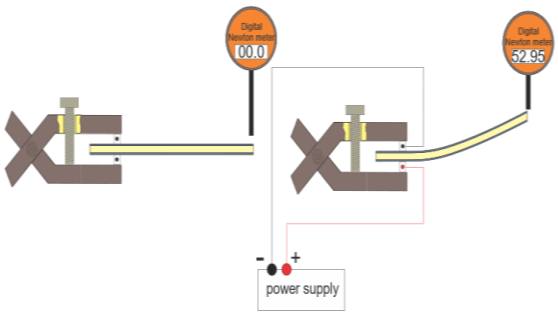

Fig. 1. Measuring the blocking force produced by IPMC (with units of $10^{-3}\ N$)

In this research, we study the generated blocking force, and its magnitude and see if it can tolerate the weight of a specimen as a gripper.

After the production procedure explained in the previous section, we have an IPMC sample that could be cut into pieces with the desired dimensions. Two pieces of IPMC with specific dimensions (see Table 1) have been constrained as cantilever beams completely parallel with each other. This structure is illustrated in Figure 2.

Applied voltages on four electrode layers of this set are applied in such a way that Two surfaces facing each other from two different samples have a positive charge and external surfaces have a negative charge or in other words, they are ground; thus the IPMC samples deform such that equipotential surfaces get close to each other. In this case, the gripper is built.

We put a spherical aluminum sample with a radius of $8.23\times10^{-4}\ m$, between the gripper's arms. The blocking force generated by the IPMC arms is applied perpendicularly to the surface of the sphere. If the friction force between the gripper arms and the spherical body, overcomes the sample weight, the IPMC gripper could lift and move the sample. Dimensions, weight, and properties of the spherical samples are listed in Table 3.

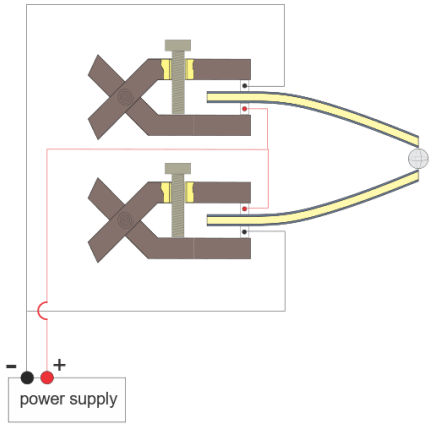

Fig. 2. Structure of the IPMC gripper

We need to measure the generated blocking force of IPMC's arms for verification and comparison of the results; for this purpose, we use a dynamometer to measure the blocking force of an IPMC sample (one of the gripper's arms).

How to use this dynamometer is given in Figure 1. The result of this measurement shows that the magnitude of the blocking force is $52.95\times10^{-3}\ N$. Considering this result, we explain the finite element method in the following section.

The ASTM standard E74 outlines the calibration procedures for force-measuring instruments used in testing machines and

laboratories. It ensures that force measurements are traceable to the SI unit of force. Users, manufacturers, and calibration laboratories need this standard to maintain accurate and reliable force measurements in various applications. In this research, all force measurements have been conducted according to this ASTM standard.

Including the coefficient of friction in the analysis of Ionic Polymer-Metal Composites (IPMCs) increases the accuracy in the prediction of their performance in real-world applications, such as microgrippers. Considering friction, more precise and reliable results can be achieved. To measure this coefficient a device like a tribometer should be used to apply a known force and then calculate how much force is needed to slide the object. Dividing this force by the normal force will result in the coefficient of friction. Doing several tests and considering factors like temperature and humidity will ensure more accurate results. In this research, the coefficient of friction is not measured directly; instead, it is achieved by taking into account several amounts and choosing the closest one to the experimental results (measured blocking force).

2.3. Finite element method

The second analysis method used in this research is the finite element method. In this research, the finite element method is performed under two stages; one for calculating the magnitude of blocking force generated by IPMC with identical dimensions and properties with the produced sample used in experimental analysis and one for calculating the induced stress on the external sample and its deformation, and evaluating the ability of IPMC gripper in lifting and moving the specific sample with specified properties. These two stages are going to be discussed in the following.

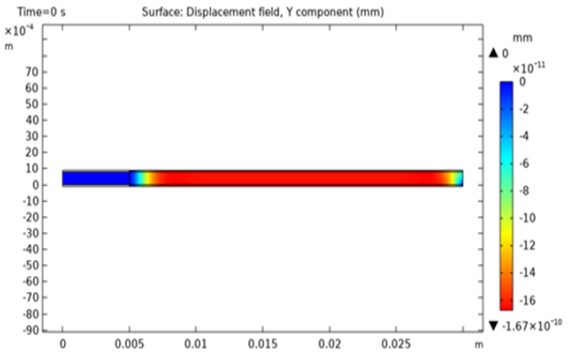

Fig. 3. Displacement of the ionic polymer metal-composite under the proposed support constraints

After simulating the geometry of IPMC and setting the required physics for that, a uniform mesh was applied to both the polymeric layer and electrodes; then the boundary conditions were applied when the base of the IPMC was fixed and a uniform voltage was applied to the electrode surfaces. This mimicked the real-life activation process. It is undeniable that there is friction force present between IPMC's electrodes and external specimens; therefore a friction coefficient was considered for an accurate simulation of IPMC's interaction with external specimens. A time-dependent solver with 0.1-second intervals was chosen to capture the dynamic response over time. This solver appropriately calculated the nonlinear behavior of the IPMC, including both its electromechanical and mechanical properties. All these configurations resulted in a thorough investigation of how the IPMC affects stress and deformation in external specimens.

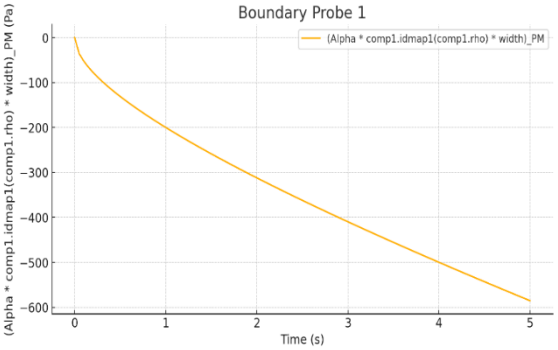

Fig. 4. Maximum force per unit area of ionic polymer metal-composite versus time

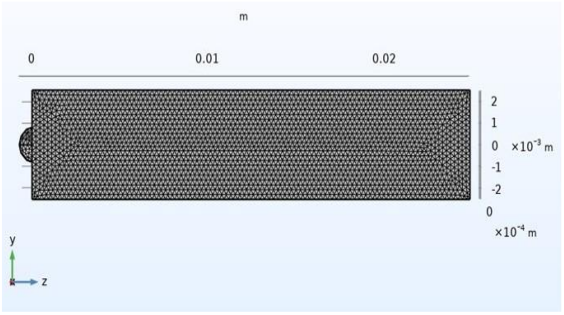

(a)

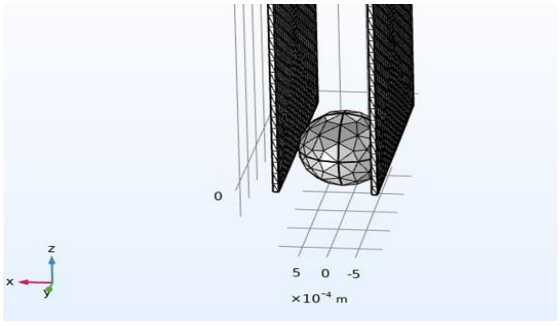

(b)

Fig. 5. Meshing of the external specimen, along with the contact surface of the ionic polymer metal composite with the sphere (a) up view, (b) Isometric view

As was described, the first stage aims to calculate the magnitude of blocking force generated by IPMC. For this purpose, the properties and specifications of the IPMC were set in finite element software. The dimensions, including the thickness of the electrodes and polymer layers, were then applied to the geometry, and the relevant physical constraints were simulated. As the final step, the geometry is meshed. Three volts of voltage are applied to the electrode surfaces. The FEM analysis is time-dependent from $0\,s$ to $5s$ and with intervals of $0.05\,s$. The finite element software provides the desired results by solving the electrochemical and physical related equations; these equations are thoroughly described in the Theory section. Parameters related to IPMC's properties, geometry, and dimensional specifications are listed in Table 3.

Based on this analysis, a distributed load is generated and it is applied to the unit surface of the composite. The magnitude of this force is almost constant based on Figure 3 (ignoring the minor force changes at the fixed end of the beam). According to this diagram, the magnitude of the distributed load is approximately equal to $590\ N/m^2$ The surface area of the sample is equal to $115\,mm^2$. After conducting the statistical calculations, the concentrated force on the tip of the beam is $52.95 \times 10^{-3}\ N$ .Figure 4 illustrates the maximum force generated per unit area of the composite over time; according to this diagram, it is observable that the magnitude of this distributed load reaches the constant amount of $590\,N/m^2$ through time. Specifications of applied mesh on the IPMC are listed in Table 2.

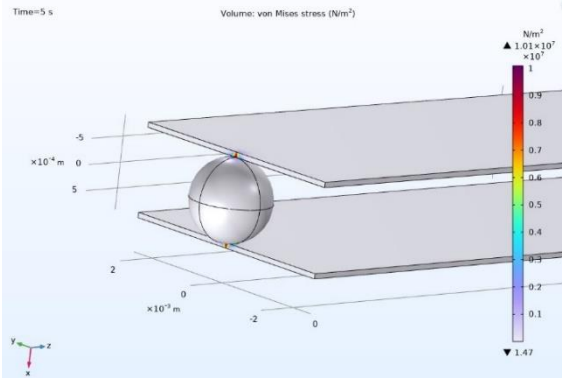

Fig. 6. The stress applied on the aluminum specimen, under the influence of blocking force produced by the ionic polymer metal-composite

The mentioned second stage of FEM analysis is for calculating the induced stress on a spherical specimen and measuring its deformation. Two different materials are considered for this purpose; pure aluminum and some fish's eggs (since the IPMC is a biocompatible material). Specifications of applied mesh on this external specimen are listed in Table 4 and these properties are identical for both considered materials.

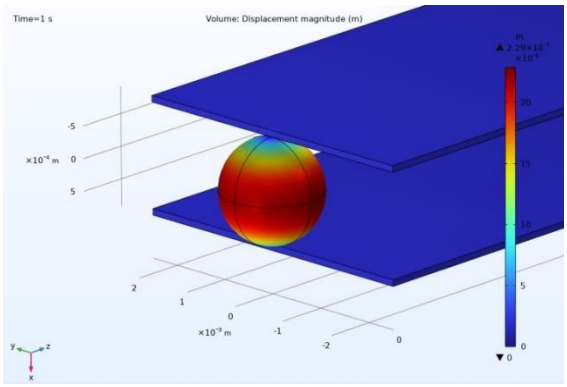

Fig. 7. Displacement of the aluminum specimen under the influence of blocking force produced by the ionic polymer metal composite

In this stage, we should consider the effect of friction force between the spherical specimen's surface and electrode surface. As it is distributed in Figure 5, two layers of the electrode are in touch with the specimen's surface. We know that coated layers of platinum on the polymeric layer, are in the form of nanoparticles; so the mechanical properties of these layers, including Young's modulus, Poisson's ratio, and density differ from the standard sample of platinum bullion. These amounts are listed in Table 3 and are approximately 11.9% less than standard.

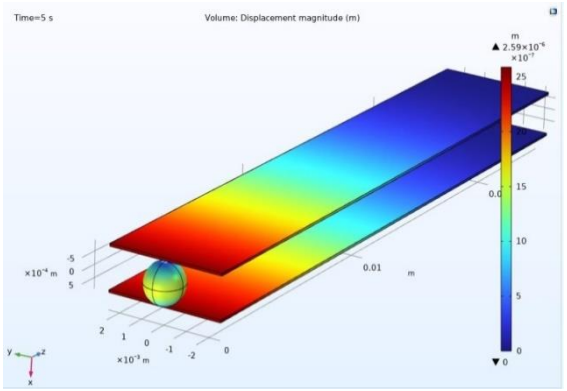

Fig. 8. Displacement of a fish egg sample under the influence of blocking force produced by the ionic polymer metal-composite

The dominance of the weight of the specimen over the static friction force between the surface of the specimen and the surfaces of the electrodes is essential for lifting and moving it. The coefficient of static friction (μ_s) is 0.2.

In the second stag9e, by applying this concentrated force to the spherical sample, and taking into account the sample's weight and the static friction force, it is observed that the maximum stress on the spherical sample is

identical for both materials (pure aluminum and fish egg) and it is equal to 9.97 Mpa. Under the influence of concentrated force, the maximum displacement observed for the aluminum sample is equal to 0.613 μm and for the fish egg sample, it is equal to 2.62 μm. Figures 8 and 9, show the amount of displacement and the applied stress on the fish egg, respectively, and Figures 7 and 6, are the corresponding figures for pure aluminum.

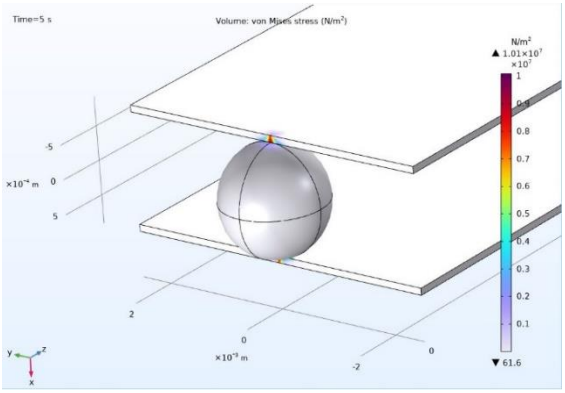

Fig. 9. The applied stress on a fish egg sample, under the influence of blocking force produced by the ionic polymer metal-composite

Table 1. IPMC's Parameters and dimensional properties

Parameter	Value	Unit
Diffusion coefficient	8.00×10^{11}	m^2/s
Universal Gas Constant	8.312	J/mol. K
Temperature	294	K
Charge number	1	
Cation concentration	1300	mol/m^3
Permittivity	2	mF/m
Faraday constant	96485.3415	C/mol
Young's modulus	41.2	MPa
Poisson's ratio	0.495	
Density	2000	kg/m^3
Alpha	0.00012	V/m
Polymer's thickness	0.12	mm
Polymer's length	30.2	mm
Electrode's thickness	0.023	mm
Electrode's length	30.2	mm
IPMC's width	5.4	mm
Clamp length	6	mm

To understand how Ionic Polymer-Metal Composites (IPMCs) work, we simulated real-World conditions in our FEM analysis. One end of the cantilever form of IPMC was fixed, much like it would be in practical uses such as robotic grippers; besides, a constant voltage was applied across the surfaces of the IPMC to simulate how this smart material is activated in real life. To ensure our model is real, we considered the friction between the IPMC and any object it interacts with; this is a key factor for applications where precise gripping or manipulation is needed. Using a time-dependent solver helped to capture not only the immediate response but also the behavior of IPMC over time, accounting for natural tendencies like slow deformations. This study demonstrates a better prediction of how IPMCs can be applied in different technologies.

Table 2. IPMC's mesh specifications

Parameter	Value
Number of elements	10726
Maximum element size	3010
Minimum element size	5

As it was mentioned before, two spherical external specimens were considered in order to evaluate the capacity of the IPMC microgripper in moving them (pure aluminum sample and fish egg). These specimens were simulated in FEM analysis by applying each material's specifications including density, Poisson's ratio, and Young's modulus (all these details are listed in Table 3). In the next step, the sphere was fixed at the top and bottom and a friction coefficient was applied between the spherical specimen's surface and IPMC's electrode surfaces.

Table 3. Dimensions and properties of spherical samples and platinum electrodes

Value	Unit
Sphere radius	8.151×10^{-4} m
Pure aluminum Poisson's ratio	0.35
Pure aluminum young modulus	79.1 GPa
Pure aluminum density	$2.72\ g/cm^3$
Fish egg's Poisson's ratio	0.3
Fish egg's young modulus	0.2201 GPa
Fish egg's density	$1.0202\ g/cm^3$
Layer of Platinum particles Poisson's ratio	0.3344
Layer of Platinum particles young modulus	139.701 GPa
Layer of Platinum particle density	$18.8759\ kg/m^3$

Table 4. Spherical samples mesh properties.

Parameter	Value
Tetrahedra	28518
Triangles	19102
Number of elements	28518
Element volume ratio	0.017625
Mesh volume	2.809×10^{-8} m^3
Maximum element size	0.00207
Minimum element size	2.528×10^{-4}
Maximum element growth rate	1.45

3. Theory

In the case of water-based ionic polymer metal-composites, migrating cations attract water molecules and cause osmotic pressure changes, resulting in swelling of the polymer near the cathode and shrinkage near the anode. This, in turn, causes the material to bend towards the anode. The mechanoelectrical phenomenon is the inverse of the electromechanical phenomenon. A voltage is induced across the polymer, between the electrodes, in response to an applied deformation. It is important to understand that the main cause of both phenomena is the induced ionic current and the non-zero spatial charge in the vicinity of the electrodes. The ionic current in the polymer is calculated by using the Nernst-Planck equation [25]:

$$\frac{\partial C}{\partial t} + \nabla \cdot (-D\nabla C - z\mu FC\nabla\phi - \mu C\Delta V\nabla P) = 0 \quad (1)$$

where C is the cation concentration, μ is the mobility of the cations, D is the diffusion constant, F is the Faraday constant, z is the charge number, ΔV is the molar volume, which quantifies the hydrophilicity of the cation, P is the solvent pressure, and ϕ is the electrical potential in the polymer. Mobility can be expressed explicitly as follows [26]:

$$\mu = \frac{D}{RT} \quad (2)$$

where R is the gas constant and T is the absolute temperature. The main governing equation, equation (1), is used to describe the transfer phenomenon of ionic polymer metal composites.

3.1. Finite Element Method

The modified PNP equation includes additional factors such as charged membranes, finite-size ions, and so on. These modifications cause better capturing of the ion's behavior in complex environments.

Depending on the system under consideration, the specific form of the modified PNP equation varies. Often, additional terms are involved to account for factors like ion size, ion-ion interactions, steric effects, or the presence of charged interfaces [27].

Overall, a framework for understanding and predicting the behavior of ions in diverse environments like biological cells and electrochemical devices is provided by the modified PNP equation. It is practical in fields such as biophysics, electrochemistry, and materials science.

When evaluating the electrochemical response using a spatially one-dimensional model along the membrane thickness we neglect the derivatives of ψ, C and μ in the MPNP system with respect to X. Hence the following relevant components of the electric displacement and counterion flux are presented [28]:

$$D_Y = -\frac{\epsilon\left(1 + (\varphi_m{}')^2 Y^2 - 2\varphi_m{}' Y\cos(\varphi - \varphi_m)\right)}{J}\frac{\partial\psi}{\partial Y} \quad (3)$$

$$J_Y = -\frac{D}{J^2}\left(1 + (\varphi_m{}')^2 Y^2 - 2\varphi_m{}' Y\cos(\varphi - \varphi_m)\right) \times \left(\frac{C}{J}\varphi_m{}' + \frac{\partial C}{\partial Y} + \frac{F}{RT}C\frac{\partial\psi}{\partial Y}\right) \quad (4)$$

with J the volume ratio. Here, invariably with the finite deformation finite element (FE) analyses, it is assumed that the distributed load p acts along the Y direction all along the loading history, and we have $y = y_0$. For this reason, we use this relation: $\varphi = \arcsin(v')$. In particular, the flux has three main contributions proportional to $\varphi_m{}'$, $\frac{\partial C}{\partial Y}$ and $\frac{\partial\psi}{\partial Y}$. It should be noted that the curvature, $-\varphi_m{}'$, is the through-the-thickness component of the volume ratio gradient. In the flux (equation (4)), it is also modulated by the shear deformation $\varphi - \varphi_m$.

Just after the application of the mechanical load, at $t = 0^+$, the IPMC state is approximated by [29]:

$$C \approx C_0, \frac{\partial C}{\partial Y} \approx 0, \frac{\partial\psi}{\partial Y} \approx 0 \quad (5)$$

It corresponds to negligible counterion migration which is related to the electrophoretic effect, while diffusion which is associated with Fick's law results in the electrochemical response [30].

$$J_Y \approx -D(1 + \sin^2(\varphi - \varphi_m)J^2)\frac{C_0}{J}\varphi'_m \quad (6)$$

Equation (6) shows that the electrochemical response vanishes in the absence of curvature. Because both $\sin^2(\varphi - \varphi_m) \geq 0$ and J decreases with increasing $-\varphi_m$, the shear deformation amplifies the electrochemical response.

Equation (4) particularizes to the analogous relation obtained in Porfiri et al and membrane shear deformation is neglected.

The Modified Poisson-Nernst-Planck (MPNP) system can be expressed as follows [31]:

$$-\varepsilon \frac{\partial}{\partial Y}\left[\frac{1+(\varphi_m')^2 Y^2 - 2\varphi_m' Y \cos(\varphi-\varphi_m)}{J}\frac{\partial \psi}{\partial Y}\right] = F(C - C_0) \quad (7)$$

$$\frac{\partial C}{\partial t} = D\frac{\partial}{\partial Y}\left[\frac{1+(\varphi_m')^2 Y^2 - 2\varphi_m' Y \cos(\varphi-\varphi_m)}{J^2} \times \left(\frac{C}{J}\varphi_m{}' + \frac{\partial C}{\partial Y} + \frac{F}{RT} C \frac{\partial \psi}{\partial Y}\right)\right] \quad (8)$$

and the following boundary and initial conditions are considered [32]:

$$\psi(\pm H, t) = 0, t \geq 0 \text{(short circuit)} \quad (9)$$

$$J_Y(\pm H, t) = 0, t \geq 0 \text{(ion-blocking)} \quad (10)$$

$$\psi(Y,0) = 0 \text{ and } C(Y,0) = C_0, \quad Y \in [-H, H] \text{(electroneutrality)} \quad (11)$$

Additionally, integrating the Poisson and Nernst-Planck equations, while considering ion-blocking and electroneutrality conditions, reveals that [33]:

$$D_Y(H,t) = D_Y(-H,t) = -Q \quad (12)$$

Q denotes the stored charge per unit nominal area, and its time derivative is the electric current per unit nominal area [34]:

$$I = \frac{dQ}{dt} = -\frac{dD_Y(\pm H, t)}{dt} \quad (13)$$

4. Discussion

Previous research has explored the use of an IPMC strip in a microgripper designed for handling miniature components on the micro-scale. The IPMC strip provides deflection and force response suitable for holding and lifting flexible tiny components without conventional motors. A customized control system ensures uniform grasping force; also the experimental analysis demonstrates the system's effectiveness at room temperature. This advantage offers potential energy, space, and resource savings in downsized production systems [35].

Another study introduces a novel design of an IPMC-based micro gripper actuated by EMG signals obtained from human fingers. Controlling the gripper is effectively done by the EMG data in an open-loop system. A PID control system is employed to ensure stability during finger operation. Deflection and load analysis shows that the IPMC gripper can achieve significant deflection and lift capacity. The IPMC exhibits capacitive and resistive behavior; these behaviors pave the way for the development of a microgripper using EMG signals. Pin insertion during robotic micro assembly operations is one of this gripper's applications. Future work may involve enhancing the gripper's capabilities for peg-in-hole assembly tasks by EMG-controlled artificial human fingers or hands [36].

During research on a highly stable air-operating IPMC actuator with consecutive channels, copper foam was introduced and removed, and microchannels and nanopores were created in the Nafion membrane. This structure enhanced ionic liquid absorption, resulting in higher capacitance and improved actuation stability. The porous IPMC exhibited significant blocking force, and strain, and is able to operate for over 180,000 cycles. Additionally, successful grasping of various objects has been observed by a soft gripper using micropillar dry adhesive on the porous IPMC surface. This porous actuator holds promise for applications in bio-inspired actuators, artificial muscles, and soft robots due to its unique capabilities and performance [37].

Developing mathematical models to predict actuation force and displacement for IPMC actuators in a PDMS-based microgripper has been focused on. For achieving higher force and displacement, these models emphasize the importance of voltage and frequency parameters, as well as the use of KCl dopant and doping solutions to enhance these properties. Through Multi-Criteria Decision Making techniques, shows that PDMS is the ideal material for the compliant gripper. Compatibility between the IPMC actuator and PDMS gripper is assessed before fabrication. The resulting microgripper successfully handles small objects weighing 1.239 g [38].

An innovative IPMC gripper combining actuation and sensing capabilities is introduced in another research. Using a Hammerstein model to address its nonlinear behavior, a control strategy is devised. A novel control scheme is proposed, integrating inverse creep compensation for static nonlinearity and robust control for dynamic behavior. Experimental results confirm that the control system in ensuring stable manipulation is effective,

particularly in hybrid force and position control [39].

A novel design and fabrication method for an IPMC microgripper is represented aiming to address challenges in handling small, delicate objects. The gripper achieves precise actuation characteristics by utilizing micro-structured IPMC strips fabricated through laser beam machining. A hand-shaped design with specific dimensions is determined, enabling the gripper to capture objects within 0.5 seconds. The gripper has interlocking fingers, that allow it to hold objects with diameters of up to 2 mm and weights of up to 1.239 g. Successfully grasping small, irregular-shaped objects such as starfish-shaped acrylic stones and even fruit flies demonstrates practical applications [40].

Since environmental issues are a controversial and important topic these days and people have become more aware of them, scientists are working harder to find ways to reduce our dependency on traditional plastics. A new area of research focuses on creating new types of plastics from sustainable sources such as plants; these materials can break down easily and don't cause any harmful impacts on the environment. A cleaner, greener future can be the result of using these biodegradable materials. [41]

Another study shows the influence of various sizes of teak wood dust particles on the strength and heat resistance of polyester. According to this research, it is concluded that while adding more dust usually reduces these properties, larger dust particles help improve them. The computer simulation was used to confirm the results. [42]

According to a study about epoxy, it was found that adding walnut shell powder (WSP) to epoxy can improve its durability. Researchers found that mixing different amounts of WSP (5%, 10%, and 15%) results in more resistance to wear on epoxy. They used special tests and computer models to find out various factors affecting this improvement. [43]

Jute and Kevlar fibers are tested in vinyl epoxy composites. It was found that a stacking sequence of four layers of Kevlar (KKKK) provides the best mechanical properties; Kevlar-Jute-Kevlar-Jute (KJKJ) sequence also performs well. [44]

Epoxy composites containing LD sludge demonstrate the highest strength and wear resistance. The increase of LD sludge content to 16% wt. boosts strength by up to 15%. The main factors that influence wear are the quantity of LD sludge and the testing speed. [45]

In this research a novel application of the finite element method (FEM) is presented; two stages are considered for this analysis (analysis of the generated blocking force of Ionic Polymer-Metal Composites (IPMCs) and its influence on different materials, including biocompatible ones such as fish eggs). Another unique exploration in this research is the mechanical behavior of IPMCs and evaluation of their potential application in precise tasks, especially in biomedical fields. This work is significant since it contributes to understanding IPMC performance and it offers practical insights when it comes to device design and optimization; it also highlights potential uses in biomechanics and delicate handling.

5. Results

The second analysis method used in this research is the finite element method. In this research, the finite element method is performed under two stages; one for calculating the magnitude of blocking force generated by IPMC with dimensions and properties identical to the produced sample used in the experimental analysis and one for calculating the induced stress on the external specimen and its deformation, and evaluating the ability of IPMC gripper in lifting and moving the specific sample with specified properties. These two stages are going to be discussed in the following paragraphs.

As was described, the first stage aims to calculate the magnitude of blocking force generated by IPMC. The magnitude of external voltage applied on the electrode surfaces is 3 V (similar to the experimental analysis). The FEM analysis is time-dependent from 0 s to 5 s and with intervals of 0.1 s. The finite element software provides the desired results by solving the electrochemical and physical related equations.

Based on this analysis, a distributed load is generated and it is applied to the unit surface of the composite. The magnitude of the distributed load is approximately equal to $848.9 N/m^2$. The surface area of the sample is equal to 115 mm^2. After conducting the statistical calculations, the concentrated force on the tip of the beam is equal to 52.95×10^{-3} N. The magnitude of this distributed load reaches the constant amount of 590 N/m^2 through time.

The mentioned second stage of FEM analysis is for calculating the induced stress on a spherical specimen and measuring its deformation. Two different materials are considered for this specimen; pure aluminum and some fish's eggs (since the IPMC is a biocompatible material).

In this stage, we should consider the effect of friction force between the spherical specimen's surface and electrode surface. Two layers of the electrode are in touch with the specimen's surface.

In the second stage, it is observed that the maximum stress on the spherical sample corresponds to both types of materials (pure aluminum and fish egg) and it is equal to 9.97 Mpa. Under the influence of concentrated force, the maximum displacement of the aluminum sample is equal to 0.613 μm and for the fish egg's sample, it is equal to 2.62 μm.

A number of challenges and considerations must be considered when scaling up the size of an Ionic Polymer-Metal Composite actuator. More power is required for larger actuators and material inconsistencies might affect the material's performance in that case. Larger IPMCs may respond more slowly because of increased mass; it is also crucial to control expected overheating which is a mighty result of higher applied voltages. Last but not least, the higher costs of manufacturing larger samples of IPMCs are significant and must be considered.

6. Conclusions

Evaluating the electromechanical behavior of an IPMC with specific properties as an actuator and in application of a gripper was the purpose of this research. Two analysis methods have been used and the results have shown the magnitude of maximum blocking force generated by the IPMC with electrical excitation of 3 V, the maximum stress induced on two spherical samples (with a radius of $8.23 \times 10^{-4}\ m$), and their deformation under this applied stress. According to references, the magnitude of the yield stress of aluminum is equal to 40 Mpa, and the magnitude of the yield stress of the fish egg sample with the specifications mentioned in this research is equal to 30.3 Mpa; By comparing these values with the amount of stress on the foreign body sample, which was equal to 9.97 Mpa ($52.95 \times 10^{-3}\ N$ of concentrated force was produced on the tip of the IPMC strips)for both types of external samples, it can be concluded that the stress applied by the ionic polymer metal-composite on the spherical specimens due to the blocking force is less than the tolerable stress threshold; it is for both samples and as a result, there is no deformation or failure. The results obtained in the finite element method and the experimental method have an acceptable agreement with each other, hence, it can be concluded that the obtained results are acceptable and correct. It is also observed that IPMC with the dimensions of 115 mm^2, under the influence of 3 V voltage produces a force on the scale of $10^{-3}\ N$. By comparing the magnitude of the force obtained by the experimental method and the finite element method, the error percentage of this research is equal to 0.092 %. According to our prediction, future research on IPMC actuators will likely introduce better materials to make IPMCs more durable and responsive; besides, finding a way to miniaturize them can be another approach (for use in tiny devices). It is also possible that future research focuses on combining IPMCs with other smart materials to manufacture multifunctional devices. IPMCs are biocompatible materials, therefore, more focus can be put on making IPMCs safer for use in the body and exploring applications including soft robotics surgery tools.

Nomenclature

μ	Mobility of the cations
D	Diffusion constant
R	Gas constant
T	Absolute temperature
φ	Phase in frequence domain
ψ	Field potential
J	Volume ratio
C	Cation concentration
ε	Permittivity
t	Time
Q	Stored charge per unit nominal
F	The Faraday constant
I	electric current per unit nominal area
μ_s	The coefficient of static friction

Acknowledgments

Gratitude is extended to all those who provided support throughout the research process. Special thanks are given to the advisor for guidance and insightful suggestions. Colleagues are also acknowledged for their assistance and constructive feedback.

Funding Statement

This research did not receive any specific grant from funding agencies in the public, commercial, or not-for-profit sectors.

Conflicts of Interest

The author declares that there is no conflict of interest regarding the publication of this article.

References

[1] Khan, M., Li, T., Hayat, A., Zada, A., Ali, T., Uddin, I., Hayat, A., Khan, M., Ullah, A., Hussain, A. and Zhao, T., 2021. A concise review on the elastomeric behavior of electroactive polymer materials. *International Journal of Energy Research, 46* (15), pp.14306–14337.

[2] Dong, Y., Yeung, K.W., Tang, C.Y., Law, W.C., Tsui, G.C.P. and Xie, X., 2021. Development of ionic liquid-based electroactive polymer composites using nanotechnology. *Nanotechnology Reviews, 10*, pp. 99–116.

[3] Maksimkin, A.V., Dayyoub, T., Telyshev, D.V. and Gerasi-menko, A.Y., 2022. Electroactive polymer-based composites for artificial muscle- like actuators: A review. *Nanomaterials, 12*, p. 2272.

[4] Tsiakmakis, K., Delimaras, V., Hatzopoulos, A.T., and Papadopoulou, M.S., 2023. Real time discrete optimized adaptive control for ionic polymer metal composites. *WSEAS Transactions on Systems and Control, 18*, pp. 26–37.

[5] Nasrollah, A., Soleimanimehr, H. and Khazeni, H., 2021. Nafion-based ionic-polymer-metal composites: displacement rate analysis by changing electrode properties. *Advanced Journal of Science and Engineering, 2*, pp.51–58.

[6] Yang, L., Wang, H., and Zhang, X., 2021. Recent progress in preparation process of ionic polymer-metal composites. *Results in Physics, 29*, p. 104800.

[7] Barbero, E. J., 2023. *Finite Element Analysis of Composite Materials using Abaqus*. CRC press.

[8] Zoski, C.G., 2006. *Handbook of electrochemistry*. Elsevier.

[9] Tozzi, K.A., Goncalves, R., Barbosa, R., Saccardo, M.C., Zuquello, A., Sgreccia, E., Narducci, R. Scuracchio, C.H. and di Vona, M.L., 2023. Improving electrochemical stability and electromechanical efficiency of ipmcs: tuning ionic liquid concentration. *Journal of Applied Electrochemistry, 53*, pp. 241–255.

[10] Nic, M., Jirat, J. and Kosata, B., 2005. *compendium of chemical terminology.* International Union of Pure and Applied Chemistry.

[11] NIST, 2025. *Fine-structure constant.* The nist reference on constants, units, and uncertainty. Availabe at : https//physics.nist.gov/cgi-bincuu/value (Accessed: 2025).

[12] NIST, 2025. *Vacuum electric permittivity.* The nist reference on constants, units, and uncertainty. Availabe at : https//physics.nist.gov/cgi-bincuu/value (Accessed: 2025).

[13] NIST, 2025. *Density of material.* The nist reference on constants, units, and uncertainty. Availabe at : https//physics.nist.gov/cgi-bincuu/value (Accessed: 2025).

[14] Ling, B., Wei, K., Wang, Z., Yang, X., Qu, Z. and Fang, D., 2020. Experimentally program large magnitude of poisson's ratio in additively manufactured mechanical metamaterials. *International Journal of Mechanical Sciences, 173*, p. 105466.

[15] Lv, W. Li, D. and Dong, L., 2021. Study on blast resistance of a composite sandwich panel with isotropic foam core with negative poisson's ratio. *International Journal of Mechanical Sciences, 191*, p. 106105.

[16] Bernat, J., Gajewski, P., Ko-lota, J. and Marcinkowska, A., 2023. Review of soft ac-tuators controlled with electrical stimuli: Ipmc, deap, and mre. *Applied Sciences, 13*, p. 1651.

[17] Chang, L., Wang, D., Hu, J., Li, Y., Wang, Y. and Hu, Y., 2021. Hierarchical struc- ture fabrication of ipmc strain sensor with high sensitivity. *Frontiers in Materials, 8*, p. 748687.

[18] Nasrollah, A., Soleimanimehr, H. and Haghighi, S.B., 2024. Ipmc-based actuators: An approach for measuring a linear form of its static equation. *Heliyon, 10*(4), e24687.

[19] Ragot, P.M., Hunt, A., Sacco, L.N., Sarro, P.M. and Mastrangeli, M., 2023. Manufacturing thin ionic polymer metal composite for sensing at the microscale. *Smart Materials and Structures, 32*, p. 035006.

[20] Kim, K.J., and Shahinpoor, M., 2003. Ionic polymer–metal composites: II. manufacturing techniques. *Smart materials and structures, 12*, p.65.

[21] Yu, M., Shen, H. and Dai, Z.d., 2007. Manufacture and performance of ionic

polymer-metal composites. *Journal of Bionic Engineering, 4*, pp. 143–149.

[22] Khmelnitskiy, I.K., Vereschagina, L.O., Kalyonov, V.E., Lagosh, A.V. and Broyko, A.P., 2017. Improvement of manufacture technology and investigation of ipmc actuator electrodes. i*n 2017 IEEE Conference of Russian Young Researchers in Electrical and Electronic Engineering* (pp. 892–895).

[23] Sarkis, S., 2022. *3D Printing of IPMC Actuators Based on the Direct Assembly Method* (Doctoral dissertation, the Lebanese American University).

[24] Pugal, D., Kim, S., Kim, K. and Leang, K., 2010. Ipmc: recent progress in modeling, manufacturing, and new applications. *Electroactive Polymer Actuators and Devices*, pp.228–237.

[25] Jasielec, J.J., 2021. Electrodiffusion phenomena in neuroscience and the nernst–planck–poisson equations. *Electrochem, 2,* pp. 197–215.

[26] Olsen, Z.J. and Kim, K.J., 2021. A hyperelastic porous media framework for ionic polymer-metal composite actuators and sensors: thermodynamically consistent formulation and nondimensionalization of the field equations. *Smart Materials and Structures, 30*, p. 095024.

[27] Yang, J., Janssen, M., Lian, C. and Van Roij, R., 2022. Simulating the charging of cylindrical electrolyte-filled pores with the modified poisson–nernst–planck equations. *The Journal of Chemical Physics, 156*.

[28] Dolatabadi, R., Mohammadi, A. and Baghani, M., 2021. A computational simulation of electromembrane extraction based on poisson-nernst-planck equations. *Analytica Chimica Acta, 1158*, p. 338414.

[29] Zhang, L. and Liu, W., 2020. Effects of large permanent charges on ionic flows via poisson–nernst–planck models. *SIAM Journal on Applied Dynamical Systems, 19*, pp. 1993–2029.

[30] Wen, Z., Zhang, L. and Zhang, M., 2021. Dynamics of classical poisson–nernst–planck systems with multiple cations and boundary layers. *Journal of Dynamics and Differential Equations, 33*, pp. 211–234.

[31] Wen, Z., Zhang, L., Zhang, M., 2021. Dynamics of classical poisson–nernst–planck systems with multiple cations and boundary layers. *Journal of Dynamics and Differential Equations, 33*, pp. 211–234.

[32] Wen, Z., Bates, P.W. and Zhang, M., 2021. Effects on i–v relations from small permanent charge and channel geometry via classical poisson–nernst–planck equations with multiple cations. *Nonlinearity, 34*, p. 4464.

[33] Liu, J.L. and Eisenberg, B., 2020. Molecular mean-field theory of ionic solutions: A poisson-nernst-planck-bikerman model. *Entropy, 22*, p. 550.

[34] Gwecho, A.M., Wang, S., Mboya, O.T., 2020. Existence of approximate solutions for modified poisson nernst-planck describing ion flow in cell membranes. *American Journal of Computational Mathematics, 10*, p. 473.

[35] Jain, R. K., Datta, S., Majumder, S. and Dutta, A., 2011. Two ipmc fingers based micro gripper for handling. *International Journal of Advanced Robotic Systems, 8*, p. 13. arXiv:https://doi.org/10.5772/10523.

[36] Jain, R., Datta, S. and Majumder, S., 2013. Design and control of an ipmc artificial muscle finger for micro gripper using emg signal. *Mechatronics, 23*, pp. 381–394.

[37] He, Q., Liu, Z., Yin, G., Yue, Y., Yu, M., Li, H., Ji, K., Xu, X., Dai, Z. and Chen, M., 2020. The highly stable air-operating ionic polymer metal compos- ite actuator with consecutive channels and its potential application in soft gripper. *Smart Materials and Structures, 29*, p. 045013.

[38] Bhattacharya, S., Tiwary, P., Shayaque, A., Bepari, B. and Bhaumik, S., 2020. Anticipation of actuation properties of ipmc for soft robotic gripper. In *2nd International Conference on Communication, Devices and Computing* (pp. 405–416).

[39] Wang, H., Gao, J., Chen, Y. and Hao, L., 2021. Hammerstein modeling and hybrid control of force and position for a novel integration of actuating and sensing ionic polymer metal composite gripper. *Proceedings of the Institution of Mechanical Engineers, Part C: Journal of Mechanical Engineering Science, 235*, pp. 3113–3124.

[40] Shin, J., 2022. *Fabrication of Ionic Polymer Metal Composite (IPMC) Microgripper* (Doctoral dissertation, the Seoul National University Graduate School).

[41] Jena, H., Pradhan, P. and Purohit, A., 2023. Chapter 4-Dielectric properties, thermal analysis, and conductivity studies of biodegradable and biocompatible polymer nanocomposites. *In Biodegradable and*

Biocompatible Polymer Nanocomposites, pp. 113-140. Elsevier.

[42] Pradhan, P., Purohit, A., Mohapatra, S.S., Subudhi, C., Das, M., Singh, N.K. and Sahoo, B.B., 2022. A computational investigation for the impact of particle size on the mechanical and thermal properties of teak wood dust (TWD) filled polyester composites. *Materials Today: Proceedings, 63*, pp. 756-763.

[43] Pradhan, P., Purohit, A., Singh, J., Subudhi, C., Mohapatra, S.S., Rout, D. and Sahoo, B.B., 2022. Tribo-performance analysis of an agro-waste-filled epoxy composites using finite element method. *Journal of The Institution of Engineers (India): Series E, 103*(2), pp. 339-345.

[44] Purohit, A., Dehury, J., Sitani, A., Pati, P.R., Giri, J., Sathish, T. and Parthiban, A., 2024. A novel study on the stacking sequence and mechanical properties of Jute-Kevlar-Epoxy composites. *Interactions, 245*(1), p. 100.

[45] Purohit, A., Singh, S.K., and Nain, P.K.S., 2024. Analysis of mechanical and sliding wear characteristics of steel industries' solid wastes-filled epoxy composites using an experimental design approach. *MRS Advances, 9(11)*, pp. 910-915.